JOURNAL OF CHEMICAL PHYSICS VOLUME 112, NUMBER 7 15 FEBRUARY 2000

On the theory of electron transfer reactions at semiconductor electrode/liquid interfaces

Yi Qin Gao, Yuri Georgievskii, and R. A. Marcus
Noyes Laboratory of Chemical Physics, California Institute of Technology, Pasadena, California 91125

(Received 5 October 1999; accepted 23 November 1999)

Electron transfer reaction rate constants at semiconductor/liquid interfaces are calculated using the Fermi Golden Rule and a tight-binding model for the semiconductors. The slab method and a *z*-transform method are employed in obtaining the electronic structures of semiconductors with surfaces and are compared. The maximum electron transfer rate constants at Si/viologen$^{2+/+}$ and InP/$Me_2Fc^{+/0}$ interfaces are computed using the tight-binding type calculations for the solid and the extended-Hückel for the coupling to the redox agent at the interface. These results for the bulk states are compared with the experimentally measured values of Lewis and co-workers, and are in reasonable agreement, without adjusting parameters. In the case of InP/liquid interface, the unusual current vs applied potential behavior is additionally interpreted, in part, by the presence of surface states. © *2000 American Institute of Physics.* [S0021-9606(00)70507-1]

I. INTRODUCTION

Insight into the dynamics of the electron transfer reactions at semiconductor/liquid interfaces can be helpful in constructing efficient and stable photoelectrochemical cells and other applications, and is of interest in understanding the basic chemical reactions. Due to the instability and the nonideal behavior of most semiconductor electrodes in contact with liquids, only recently have reliable kinetic measurements been performed at semiconductor/electrolyte interfaces.[1–6] In these experiments the flux from the conduction band edge of a semiconductor to a molecular electron acceptor species dissolved in the solution can be expressed as

$$J_f(E)=ek_{et}n_s(E)[A], \tag{1}$$

where J_f (current per unit area) is the current density due to the direct electron transfer, e is the elementary charge, $n_s(\mathrm{cm}^{-3})$ is the electron concentration at the surface of the semiconductor and is a function of E, the applied potential, and $[A](\mathrm{cm}^{-3})$ is the concentration of the acceptors in the solution. An analogous expression can also be written for hole transfer from the valence band of the semiconductor. The units of k_{et} defined by Eq. (1) are $\mathrm{cm}^4\ \mathrm{molecule}^{-1}\,\mathrm{s}^{-1}$ and it contains the energy distribution of the electrons.

The electron transfer reactions at *n*-type Si(100)/viologen$^{2+/+}$(CH_3OH) and *n*-type InP(100)/$Me_2Fc^{+/0}$(CH_3OH) interfaces were studied systematically by Lewis group.[1,4] The built-in voltage (the voltage drop inside the semiconductor) and the concentration of the semiconductor conduction band electrons were obtained by differential capacitance vs potential measurements. The current densities were also measured as a function of the applied potential for different concentrations of acceptors and donors. The first-order dependence of current density on concentration of surface electrons n_s in the semiconductor and concentration of electron acceptors $[A]$ in the solution was verified for a series of Si/viologen$^{2+/+}$(CH_3OH) interfaces.[4] In this study[4] the authors chose a series of viologen ions with very similar molecular structures and thus presumably similar reorganization energies, but with very different free energy changes for the electron transfer reactions. The electron transfer rate constants obtained experimentally served also to measure the maximum of the electron transfer rate constant. The measured maximum rate constant for the electron transfer reaction across such an interface was in the range of $10^{-17}-10^{-16}\ \mathrm{cm}^4\,\mathrm{s}^{-1}$. The experimental studies of the electron transfer reaction at InP/$Me_2Fc^{+/0}$(CH_3OH) interfaces provided similar maximum rate constant results but less ideal voltage–current behavior.

By applying a treatment[7] for liquid/liquid interfacial electron transfer reactions to semiconductor/liquid interfaces and by assuming an ''electron ball'' model for the electron in the semiconductor, Lewis[2,8] provided a theoretical estimate of the maximum rate constant which is close to the experimental value. The treatment is closely related to the model suggested by Gerischer[9] who used a half-sphere instead of a sphere, and is a nonadiabatic approach. In the model of Lewis the electron in the semiconductor is represented by a spherical donor with radius around 10 Å, and any reorganization around the electron in the semiconductor was neglected. The electron transfer rate constant was then calculated using the formula derived for the electron transfer reactions at liquid/liquid interface,

$$k_{D,A}=\nu_n[2\pi(r_D+r_A)\beta_s^{-3}] \times e^{-(\lambda_A+\lambda_D+\Delta G^0)^2/4k_BT(\lambda_A+\lambda_D)}, \tag{2}$$

where ν_n is typically expected to be around $10^{13}\ \mathrm{s}^{-1}$ for a process which is adiabatic when the reactants are in contact, and where the decay of rate with distance through the solvent, assumed to be exponent with a decay length β_s, r_D and r_A are the radii of the donor and the acceptor, λ_D and λ_A are the reorganization associated to the donor and acceptor, and ΔG^0 is the standard free energy of the reaction in the pre-

 © 2000 American Institute of Physics

Downloaded 08 Mar 2006 to 131.215.225.174. Redistribution subject to AIP license or copyright, see http://jcp.aip.org/jcp/copyright.jsp

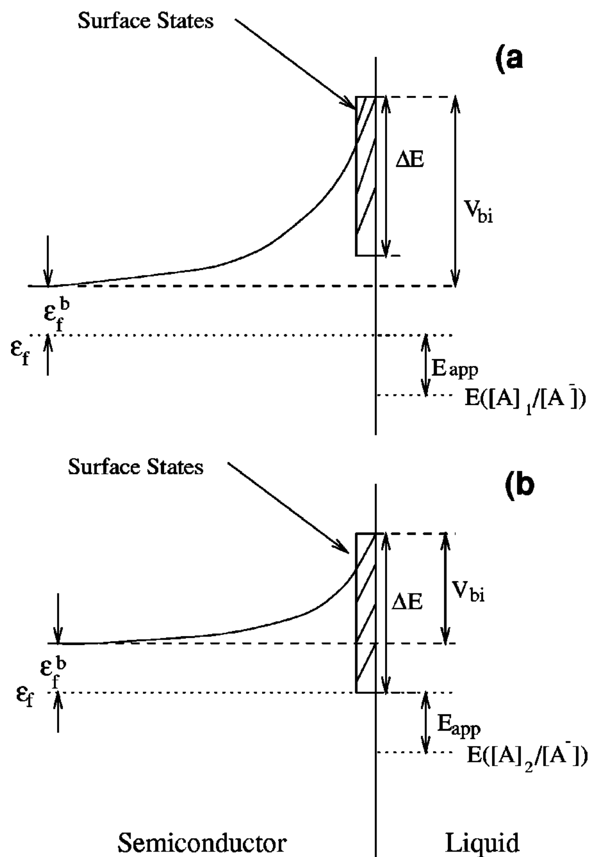

FIG. 1. The energetics at semiconductor/liquid interfaces with surface states homogeneously distributed in the energy range $(-\Delta E,0)$ referred to the conduction band edge at the surface (a) with a larger $[A]/[A^-]$ ratio and the Fermi level is far below the surface states; (b) with a smaller $[A]/[A^-]$ ratio and the occupancy of the surface states must be described by a Fermi–Dirac distribution. In (a) and (b), the same potential vs $E(A/A^-)$ is applied but (a) has a larger built-in voltage.

vailing medium. Royea, Fajardo, and Lewis[10] also investigated the relation between the electron transfer reactions at metal/liquid and semiconductor/liquid interfaces using Fermi Golden Rule. The coupling between the semiconductor and the redox molecules was not calculated for an actual system.[10]

Dogonadze and Kuznetsov[11] studied both nonadiabatic and adiabatic electron transfer reactions at semiconductor/liquid interfaces by analogy with the metal/liquid interfacial electron transfer reactions. The reorganization energy of the redox molecules at semiconductor/liquid interfaces was investigated by one of us[12] and was shown to be different from the reorganization energy for the same molecules in a homogeneous situation. Smith and Nozik[13,14] studied the semiconductor/liquid interfacial adiabatic electron transfer reactions by extending Schmickler's treatment[15] for metal/liquid electron transfer reactions, choosing an Anderson-type Hamiltonian, and by molecular dynamic calculations.[16]

In the present paper, the electron transfer reactions at semiconductor/liquid interfaces are treated nonadiabatically. Extended-Hückel calculations are performed to estimate the electronic coupling between the donor/acceptor level of the redox agent and the solid electronic states of the semiconductor. The electronic structure of the solid is treated by

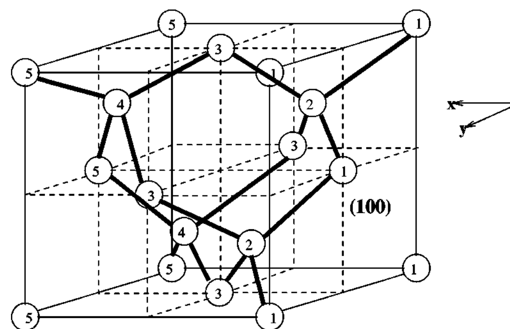

FIG. 2. View of the Si and InP semiconductor with (100) surfaces. For a Si electrode, all circles represent silicon atoms; for an InP electrode, 1,3,5,... =P and 2,4,... =In. The numbers indicate the two-dimensional layer to which the atoms belong. Every two layers of atoms form a superlayer.

tight-binding calculations using existing solid state parameters in literature, parameters that had been chosen to fit the band structure. Each semiconductor electrode is treated both as a slab and as a semi-infinite crystal for comparison. For a slab, the direct diagonalization of the Hamiltonian matrix is performed as usual to obtain the eigenvalues as well as the eigenstates,[17] while for a semi-infinite crystal, a transform method introduced earlier by one of us for this purpose[18] is employed. The procedure is applied to two semiconductor/liquid interfaces, Si/viologen$^{2+/+}$ and InP/$Me_2Fc^{+/0}$, InP/$PV^{2+/+}$. In addition, surface states are included for the current vs applied potential behavior observed at InP/$Me_2Fc^{+/0}$, $PV^{2+/+}$ interfaces, as one way for accounting for the nonideal behavior observed for this system. The maximum rate mentioned earlier, which is the principal focus of our attention, is calculated under conditions where surface states are unimportant.

The paper is organized as follows: The theoretical basis for the electron transfer rate constant calculation and solid state calculation is described in Sec. II. The application of the theoretical methods to the actual systems are given in Secs. III and IV, and the results are discussed there.

II. THEORETICAL MODELS

A. General comment

The net current density J due to the electron transfer reaction at a semiconductor S/liquid interface,

$$A+e(S)\rightleftharpoons A^-+S, \tag{3}$$

can be written as

$$J=J_f-J_r, \tag{4}$$

where J_f is the current density due to the electron transfer from the semiconductor to the molecule and J_r is the current density corresponding to the reverse process. J_f and J_r depend on the concentrations of A and A^-, respectively, at the interface,

$$J_f=ek_f[A], \tag{5}$$

$$J_r=ek_r[A^-], \tag{6}$$

Downloaded 08 Mar 2006 to 131.215.225.174. Redistribution subject to AIP license or copyright, see http://jcp.aip.org/jcp/copyright.jsp

where k_f and k_r are the first-order rate constants. In the following only the forward reaction is considered, unless otherwise stated. When it is assumed that the electron transfer from the electrode to the acceptors is proportional to the concentration of the electrons n_s at the electrode surface, in the case of an n-type semiconductor, the forward electron transfer rate constant is expressed as

$$k_f = n_s k_{et}. \tag{7}$$

Here, k_{et}, a rate constant for a reaction that is second-order with respect to the concentrations, is the quantity obtained in Lewis' experiments.

The rate of a nonadiabatic electron tunneling from one electronic state to another is frequently described by the Landau–Zener formula. Under the weak-coupling assumption, the Golden Rule expression for the nonadiabatic electron transfer rate constant, which includes both the electron tunneling and the "nuclear reorganization," contains implicitly the Landau–Zener expression,[19]

$$k_f^s = \frac{2\pi}{\hbar} |V|^2 \mathrm{FC}, \tag{8}$$

where FC is the Franck–Condon factor, V is the electronic coupling matrix element, and $\hbar$ is Planck's constant. A common classical expression for the Franck–Condon factor is[19]

$$\mathrm{FC} = \frac{1}{\sqrt{4\pi\lambda k_B T}} \exp\left(\frac{-(\lambda + \Delta G)^2}{4\lambda k_B T} \right), \tag{9}$$

where λ is the reorganization energy, and ΔG is a free energy of reaction under the prevailing conditions of temperature, electrode–solution potential difference and environment. We return later to this quantity for the present systems.

The electron transfer at the semiconductor/liquid interfaces involves the continuum of electronic states in the semiconductor, whose theory, strictly speaking, requires solving a many-electronic state problem. Quantum mechanical studies of many-state crossing problems show that the Landau–Zener formula is applicable to a large variety of such problems, when the splitting of the states caused by crossing is small.[20] The major charge carriers in a semiconductor have very low concentrations and can be treated individually in interfacial reactions.[9] In accordance with a weak-coupling approximation[20] transitions can be treated as occurring between pairs of states, and a "two-level" approximation can then be considered, in which the electron transfer current between the electrode and an acceptor state is treated as the sum of the currents from each electronic state of the electrode to the acceptor state. Considering first the acceptor as being at position $\mathbf{r}$ in the solution, the rate constant is

$$k_f^t(\mathbf{r}) = \sum_{\mathbf{k}} k_f^s(\mathbf{k},\mathbf{r}). \tag{10}$$

Here, $k_f^t(\mathbf{r})$ is the rate constant for the total current from the semiconductor to the molecule, expressed as a sum of the currents from all the electronic states of the semiconductor, $\mathbf{k}$ denotes the electronic state of the semiconductor with the wave vector $\mathbf{k}$, and $k_f^s(\mathbf{k},\mathbf{r})$ varies with the position $\mathbf{r}$ of the acceptor relative to the electrode. It can be further written as[10,11,21]

$$k_f^t(\mathbf{r}) = \frac{2\pi}{\hbar} \int_\epsilon \mathrm{FC}(\epsilon) f(\epsilon) \sum_{\mathbf{k}} |V(\mathbf{k},\mathbf{r})|^2 2\pi\delta(\epsilon_{\mathbf{k}} - \epsilon)\, d\epsilon, \tag{11}$$

where the coupling matrix element V is defined later and $f(\epsilon)$ is the probability that a state in the semiconductor with energy ϵ is occupied, while ΔG in Eq. (9) is related to ϵ by

$$\Delta G = \Delta G^0 - \epsilon. \tag{12}$$

Here, ΔG^0 is defined as the standard free energy of the reaction when the donor state in the electrode is at the conduction band edge at the semiconductor surface. ΔG^0 can be obtained from electrochemical measurements. After denoting by $\bar{V}(\epsilon,\mathbf{r})$ the averaged coupling of all the states with energy ϵ, Eq. (11) can be written as

$$k_f^t(\mathbf{r}) = \frac{2\pi}{\hbar} \int_\epsilon f(\epsilon)\rho(\epsilon)\mathrm{FC}(\epsilon) |\bar{V}(\epsilon,\mathbf{r})|^2 d\epsilon, \tag{13}$$

where $\rho(\epsilon)$ is the density of states, i.e., $\Sigma_{\mathbf{k}} 2\pi\delta(\epsilon_{\mathbf{k}} - \epsilon)$ (Ref. 22) and $|\bar{V}(\epsilon,\mathbf{r})|^2$ denotes $\Sigma_{\mathbf{k}} |V(\mathbf{k},\mathbf{r})|^2 \delta(\epsilon_{\mathbf{k}} - \epsilon) / \Sigma_{\mathbf{k}} \delta(\epsilon_{\mathbf{k}} - \epsilon)$.

The current density at the electrode is obtained by summing over the current from the electrode to all the acceptors A in the solution and dividing the sum by the area of the electrode surface σ,

$$J_f = \frac{e}{\sigma} \int_{\mathbf{r}} A(\mathbf{r}) k_f^t(\mathbf{r}) d^3\mathbf{r}, \tag{14}$$

where $A(\mathbf{r})$ is the concentration of A at $\mathbf{r}$. When the reaction is not diffusion-controlled, and when the change of electrical potential inside the liquid can be neglected, $A(\mathbf{r})$ can be taken as constant. A first-order electron transfer rate constant, which is independent of the concentration of acceptors in the solution but dependent on the concentration of electrons in the semiconductor, can be defined,

$$k_f = \frac{1}{\sigma} \int_{\mathbf{r}} k_f^t(\mathbf{r}) d^3\mathbf{r}. \tag{15}$$

When $k_f(\mathbf{r})$ depends exponentially on distance with a decay constant β_s, the k_f becomes

$$k_f = \frac{1}{\beta_s} k_f^t(\mathrm{contact}), \tag{16}$$

where $k_f^t(\mathrm{contact})$ is the value of $k_f^t(\mathbf{r})$ at the van der Waals' contact distance, averaged over orientations as discussed later in Sec. III A.

B. Tight-binding model

For obtaining the electronic states of the semiconductors, we consider the tight-binding method, which has been used extensively in treating the electronic properties of solids and their surfaces and has been useful and efficient in approximately solving solid state physics problems.[23–27] As noted earlier,[18,21,28] because it involves a linear combination of

Downloaded 08 Mar 2006 to 131.215.225.174. Redistribution subject to AIP license or copyright, see http://jcp.aip.org/jcp/copyright.jsp

atomic orbitals, the tight binding method for the electronic structure calculations for the solid is readily combined with the extended-Hückel treatment to estimate the electronic coupling at the interface.

In this approach the one-electron wave function of an infinite solid is expressed as a linear combination of Bloch functions, $\Sigma_{\mathbf{R_i}}\exp(i\mathbf{k}\cdot\mathbf{R_i})\psi_n(\mathbf{r}-\mathbf{R_i})$,

$$\Psi_{\mathbf{k}}(\mathbf{r})=\sum_n c_n(\mathbf{k})\sum_{\mathbf{R_i}}\exp(i\mathbf{k}\cdot\mathbf{R_i})\psi_n(\mathbf{r}-\mathbf{R_i}), \tag{17}$$

where $c_n(\mathbf{k})$'s are coefficients, $\psi_n(\mathbf{r}-\mathbf{R_i})$'s are atomic orbitals centered at the position $\mathbf{R_i}$, and the n's denote different bands of orbitals.

Substitution of the wave function into the Schrödinger equation, $\mathbf{H}\Psi_{\mathbf{k}}(\mathbf{r})=E_k\Psi_{\mathbf{k}}(\mathbf{r})$, produces the well known set of linear algebraic equations, with the standard result for non-trivial solutions that[23]

$$|\mathbf{H}-E\mathbf{S}|=0, \tag{18}$$

where $\mathbf{H}$ and $\mathbf{S}$ are matrices of the Hamiltonian and overlap with elements H_{nm} and S_{nm}. The elements of the matrices are readily obtained by the consideration of the symmetry of the solid and by choosing appropriate interaction and overlap parameters for the neighboring atoms, H_{nm} and S_{nm}. We have

$$H_{nm}=\sum_{\mathbf{R}_j}\exp(i\mathbf{k}\cdot(\mathbf{R_j}-\mathbf{R_i}))\int\psi_n^*(\mathbf{r}-\mathbf{R_i})\times H\psi_m(\mathbf{r}-\mathbf{R_j})d^3\mathbf{r}, \tag{19}$$

$$S_{nm}=\sum_{\mathbf{R}_j}\exp(i\mathbf{k}\cdot(\mathbf{R_j}-\mathbf{R_i}))\int\psi_n^*(\mathbf{r}-\mathbf{R_i})\times\psi_m(\mathbf{r}-\mathbf{R_j})d^3\mathbf{r}. \tag{20}$$

In practice the parameters are adjusted in the band structure calculation so as to fit experimental data on the band structure.[24] If an orthonormal basis is chosen, the $\mathbf{S}$ matrix becomes the unit matrix and Eq. (18) becomes[29]

$$|\mathbf{H}-E\mathbf{I}|=0, \tag{21}$$

where $\mathbf{I}$ is the unit matrix. The solution of the electronic structure is provided by the direct diagonalization of the Hamiltonian matrix.

An infinite solid can also be viewed as being formed by an infinite number of layers of atoms. Each of the layers has the full two-dimensional translational symmetry. In this scheme, the wave function is expressed as

$$\Psi_{\mathbf{k}}(\mathbf{r}_\parallel)=\sum_{n,m}c_{nm}(\mathbf{k}_\parallel)\sum_{\mathbf{R}_{\parallel,\mathbf{i}}}\exp(i\mathbf{k}_\parallel\cdot\mathbf{R}_{\parallel,\mathbf{i}})\psi_{nm}(\mathbf{r}_\parallel-\mathbf{R}_{\parallel,\mathbf{i}}), \tag{22}$$

where $\mathbf{k}_\parallel$ and $\mathbf{r}_\parallel$ are the wave vector and the space vector in the two-dimensional layer. Here, $\psi_{nm}(\mathbf{R}_{\parallel,\mathbf{i}})$ is the mth type atomic orbital at the position $\mathbf{R}_{\parallel,\mathbf{i}}$ in the nth layer. This wave function is easily generalized to the case where the solid is not infinite, e.g., has one (semi-infinite) or two (slab) surfaces. For a semi-infinite crystal, n, the number of the layer counted from the surface, varies from 1 to ∞. For a slab, n varies from 1 to some finite number.

In the slab method, the model of the solid is constructed using a finite number of infinite planes parallel to the surface. Each plane is composed of lattice atoms and the electronic motion in it can be described by Bloch plane waves. The one-electron wave functions of a slab consisting of N atomic layers are expanded in $M\times N$ LCAO-type Bloch functions, where M is the number of different atomic orbitals per layer for each value of $\mathbf{k}_\parallel$. The overlap and Hamiltonian matrix elements are expressed in terms of the overlap and interaction integrals between the atomic orbitals. Again, an orthonormal atomic basis can be chosen and the eigenvalues and eigenvectors can be obtained by direct diagonalization of the Hamiltonian matrix.

For a semi-infinite semiconductor, the z-transform method, which was introduced earlier for the tight-binding study of a semi-infinite solid, is applied to the present study. The detailed derivation is given in Ref. 18. In the following we consider a semi-infinite solid having M coupled bands, which arises either when an atom has several different orbitals or when each layer of the solid is a superlayer, i.e., consisting more than one layer, or both. Substitution of the wave function Eq. (22) into the Schrödinger equation yields an infinite set of difference equations. In matrix notation, the difference equations can be written as

$$\mathbf{B}^\dagger\mathbf{c_{n+2}}+(\mathbf{A}-E\mathbf{I})\mathbf{c_{n+1}}+\mathbf{B}\mathbf{c_n}=0,\quad(n\geqslant1), \tag{23}$$

$$\mathbf{B}_1^\dagger\mathbf{c_2}+(\mathbf{A}_1-E\mathbf{I})\mathbf{c_1}=0, \tag{24}$$

where $\mathbf{c_n}$ is a column vector whose elements c_{mn} describe the coefficients of the bands in the nth layer, and where

$$B_{ml}\delta(\mathbf{k}_\parallel-\mathbf{k}_\parallel')=\langle\psi_{mn}|H|\psi_{l,n-1}\rangle,\quad(n\neq1), \tag{25a}$$

$$A_{ml}\delta(\mathbf{k}_\parallel-\mathbf{k}_\parallel')=\langle\psi_{mn}|H|\psi_{ln}\rangle,\quad(n\neq1), \tag{25b}$$

$$A_{1,ml}\delta(\mathbf{k}_\parallel-\mathbf{k}_\parallel')=\langle\psi_{m1}|H|\psi_{l1}\rangle,\quad(n\neq1), \tag{25c}$$

$$B_{1,ml}\delta(\mathbf{k}_\parallel-\mathbf{k}_\parallel')=\langle\psi_{m2}|H|\psi_{l1}\rangle,\quad(n\neq1). \tag{25d}$$

Introducing the z-transform for the coefficients, defined by

$$F_m(z)=\sum_1^\infty c_{mn}z^{1-n},\quad(m=1\ \text{to}\ M), \tag{26}$$

its inversion formula is

$$c_{mn}=\frac{1}{2\pi i}\oint_C F_m z^{n-2}dz,\quad(m=1\ \text{to}\ M). \tag{27}$$

Applying them to the set of difference equations Eq. (23), and writing the result in the matrix form, we obtain

$$[z^2\mathbf{B}^\dagger+z(\mathbf{A}-E\mathbf{I})+\mathbf{B}]\mathbf{F}=[z^2\mathbf{B}^\dagger+z(\mathbf{A}-E\mathbf{I})+\mathbf{B}-\mathbf{B_1}]\mathbf{c_1}+z\mathbf{B}^\dagger\mathbf{c_2}, \tag{28}$$

with the boundary condition relating $\mathbf{c_2}$ to $\mathbf{c_1}$ given by Eq. (24).

The vector $\mathbf{F}$, whose elements are F_m, can then be obtained from Eqs. (24) and (28),

Downloaded 08 Mar 2006 to 131.215.225.174. Redistribution subject to AIP license or copyright, see http://jcp.aip.org/jcp/copyright.jsp

$$\mathbf{F}=\mathbf{I}\mathbf{c_1}-[z^2\mathbf{B}^\dagger+z(\mathbf{A}-E\mathbf{I})+\mathbf{B}]^{-1}\times[\mathbf{B_1}+z\mathbf{B}^\dagger\mathbf{B_1^\dagger}^{-1}(\mathbf{A_1}-E\mathbf{I})]\mathbf{c_1}. \quad (29)$$

As can be seen from Eq. (29), the poles of the integrand in Eq. (27) are found by locating the zeros of the polynomial

$$\det[z^2\mathbf{B}^\dagger+z(\mathbf{A}-E\mathbf{I})+\mathbf{B}], \quad (30)$$

and are used in the inversion formula to yield the coefficients c_{mn}'s in terms of c_{m1}'s. The boundary condition at the surface is included in the expression for $\mathbf{F}$, and in Eq. (29) the requirement that the wave functions do not become infinite as $n\rightarrow\infty$ is satisfied by choosing c_{m1}'s which make the terms with $|z|>1$ in Eq. (24) for c_{mn}'s vanish.

A numerically simpler way of solving the preceding problem is proposed and used here and is illustrated as follows. Since

$$\mathbf{A}^\dagger=\mathbf{A}, \quad (31)$$

in Eq. (30), z and z^{*-1} are both the zeros of the polynomial in that equation. As a result, the number of zeros inside the unit circle must equal the number of zeros outside the unit circle. By denoting the roots of z by z_l, $l=1$ to $2M$, the integral in Eq. (27) can be evaluated using Cauchy's residue theorem,

$$c_{mn}=\sum_{l=1}^{2M} z_l^{n-2}\,\mathrm{Res}\,F_m(z_l)\equiv\sum_{l=1}^{2M}\tilde{c}_{lm}z_l^{n-1}, \quad (32)$$

where

$$\tilde{c}_{lm}=z_l^{-1}\,\mathrm{Res}\,F_m(z_l). \quad (33)$$

In order to satisfy the outgoing boundary condition at $n\rightarrow\infty$, the zeros outside the unit circle are discarded by setting the corresponding $\tilde{\mathbf{c}}_\mathbf{l}$, the column vector whose elements are $\vec{c}_{lm}$, equal to zero.

Substitution of Eq. (32) into Eq. (23) yields

$$\sum_l z_l^{n+2}\mathbf{B}^\dagger\tilde{\mathbf{c}}_\mathbf{l}+\sum_l z_l^{n+1}(\mathbf{A}-E\mathbf{I})\tilde{\mathbf{c}}_\mathbf{l}+\sum_l z_l^{n+1}\mathbf{B}\tilde{\mathbf{c}}_\mathbf{l}=0. \quad (34)$$

The above equation holds for all $n\geqslant 1$, which can be satisfied by setting

$$z_l^{n+2}\mathbf{B}^\dagger\tilde{\mathbf{c}}_\mathbf{l}+z_l^{n+1}(\mathbf{A}-E\mathbf{I})\tilde{\mathbf{c}}_\mathbf{l}+z_l^{n}\mathbf{B}\tilde{\mathbf{c}}_\mathbf{l}=0, \quad (35)$$

for all z_l's. Thereby, $\tilde{\mathbf{c}}_\mathbf{l}$ is the solution of the linear system,

$$(z_l^2\mathbf{B}^\dagger+z_l(\mathbf{A}-E\mathbf{I})+\mathbf{B})\tilde{\mathbf{c}}_\mathbf{l}=0, \quad (36)$$

with boundary condition given by Eq. (24). When it can be assumed that

$$\mathbf{A}_1=\mathbf{A},\quad \mathbf{B_1}=\mathbf{B}, \quad (37)$$

the boundary condition can be rewritten as

$$\mathbf{B}^\dagger\mathbf{c_2}+(\mathbf{A}-E\mathbf{I})\mathbf{c}_1+\mathbf{B}\mathbf{c_0}=0, \quad (38)$$

with

$$\mathbf{c_0}=\sum_l \tilde{\mathbf{c}}_\mathbf{l}z_l^{-1}=0. \quad (39)$$

Upon obtaining the roots z and the corresponding coefficient vectors $\tilde{\mathbf{c}}_\mathbf{l}$, the coefficients in the wave function are readily obtained using Eq. (32). Since the system is semi-infinite, although these c_{mn}'s constitute both propagating and decaying components, the decaying wave functions go to zero as n goes to infinity and so they do not contribute to the normalization, the normalization of the wave functions only needs to be performed on the propagating ones. The wave functions are normalized to give correct number of orbitals per unit cell. For example, for a semi-infinite silicon semiconductor, there are eight $\mathbf{c_n}$'s satisfying the boundary condition. For a bulk state, each $\mathbf{c_n}$ is the linear combination of eight wave functions, at least two of which are propagating ones, and each of these wavefunctions is a linear combination of the eight atomic orbitals of the unit cell. The normalization of the $\mathbf{c_n}$'s, after taking into account the spin of the electrons, is performed in such a way that $\Sigma_m c_{mn}c_{mn}^*=2$, where the sum is over the propagating components of $\mathbf{c_n}$. The eight orthogonal wave functions satisfying the boundary conditions then give 16 orbitals per unit cell. Given the condition in Eq. (37) the final equations used in this method become equivalent to those used by Gosavi and Marcus[30] in their treatment of electron transfer at metal electrodes, although their appearance differs.

Although the above formulation of the z-transform method was derived by considering the first nearest neighbor interactions between the solid atoms, the z-transform method can be applied to the tight-binding model with interactions involving as many atoms as desired. When the interactions include more than the nearest neighbors, one can simply increase the thickness of the superlayer so that only the nearest neighboring superlayers interact with each other.

When the one-electron wave functions are expressed in an orthonormal atomic basis set, the coupling $V(\mathbf{k},\mathbf{r})$ between a solid electronic state $|\Psi_\mathbf{k}\rangle$ and the acceptor state $|\Phi\rangle$,

$$V(\mathbf{k},\mathbf{r})=\langle\Psi_\mathbf{k}|H(\mathbf{r})|\Phi\rangle, \quad (40)$$

can be expressed in terms of the couplings between the atomic states,

$$V(\mathbf{k},\mathbf{r})=\sum_{n,a,m,i,j} e^{i\mathbf{k}_\parallel\cdot\mathbf{r}_{\parallel,\mathbf{a}}}c_{nm}(\mathbf{k})^*C_{ij}\langle\psi_{nam}|H(\mathbf{r})|\phi_{ij}\rangle, \quad (41)$$

where the ϕ_{ij} is the jth orbital of the ith atom in the molecular acceptor state, and C_{ij} is the coefficient of the this orbital in forming the acceptor state, ψ_{nam} is the mth type of atomic orbital which belongs to the ath semiconductor atom in the nth layer. $\mathbf{r}_{\parallel,\mathbf{a}}$ in Eq. (41) is the position of the atom a in a semiconductor layer. We may illustrate the notation by considering a semi-infinite silicon semiconductor. Each superlayer of silicon consists of two layers of silicon atoms, and each silicon atom contains 4 relevant orbitals(e.g., $3s$, $3p_x$, $3p_y$, $3p_z$) and so m varies from 1 to 8. The first layer is formed by atoms denoted by $(1,a)$, where a is only odd numbered, 1, 3, 5,..., the orbitals of which are then denoted by $(1, a, m)$, where $m=1$, 2, 3, 4. The second layer also belongs to the first superlayer and thus $n=1$, $a=2$, 4, 6,... and $m=5$, 6, 7, 8. (We note that the $a=2$, $a=4$, etc. atoms

Downloaded 08 Mar 2006 to 131.215.225.174. Redistribution subject to AIP license or copyright, see http://jcp.aip.org/jcp/copyright.jsp

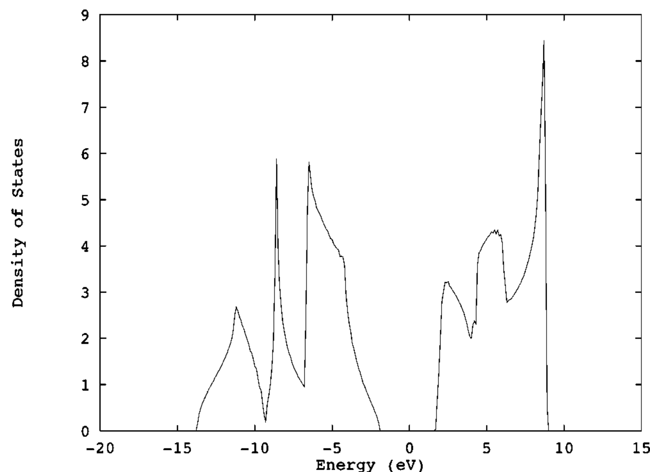

FIG. 3. Calculated density of states ρ for the bulk of Si semiconductor. The unit of the density of states is per unit cell (2 atoms) per eV. The Fermi level is located at 0 eV.

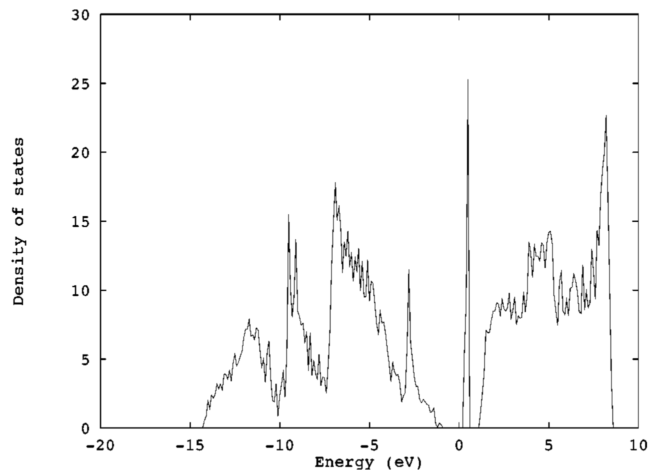

FIG. 4. Calculated density of states ρ for a slab of Si semiconductor. The unit of the density of states is per eV per unit cell. There are 20 atoms per unit cell, which has one atom on each face of the slab and so is 20 atoms thick. The Fermi level is located at 0 eV.

interact differently with the molecule, because of their different positions with respect to it.) The c_{nm} in Eq. (41) are obtained by the tight-binding calculations described earlier and are functions of $\mathbf{k}_\parallel$ but are independent of $\mathbf{r}_{\parallel,\mathbf{a}}$. The coupling matrix elements $\langle \psi_{nam}|H(\mathbf{r})|\phi_{ij}\rangle$ are obtained by the extended-Hückel calculations for the acceptor atomic orbital (i,j) and the semiconductor atomic orbital m at the position $(n,\ a)$.

III. APPLICATIONS

A. Silicon/viologen system

1. Band structure calculations of silicon

The LCAO (''tight-binding'') method has provided a good description for the semiconductor valence band and conduction band edge for silicon even when only the nearest-neighbor interactions are considered and an orthogonal basis is used.[31] In this calculation, the nearest-neighbor interaction parameters are taken from a table of solid state parameters in Ref. 25. The density of states is obtained by randomly choosing a certain number of wave vectors in the calculation which show a statistical number of the energy eigenvalues. The computed density of states for a bulk silicon is normalized to give 16 orbitals per unit cell (including the spin of the electrons) and is shown as a function of the orbital energy in Fig. 3.

The surface studied experimentally for silicon was, as noted earlier, the (100) surface. In the slab method, the silicon (100) surface bands were calculated using models of infinite silicon slabs with ideal (100) surfaces, i.e., a finite number of layers, each consisting of an infinite number of (100) silicon atoms as a two-dimensional array, are placed as in a perfect silicon crystal (Fig. 2). The one-electron wave functions are written as linear combinations of Bloch functions as in Eq. (22), where the sums are over the layers and the $3S$,$3P_x$,$3P_y$,$3P_z$ orbitals, respectively. The (100) surface is treated as ideal and the matrix elements between a Bloch function of the surface plane and one plane inside the slab is treated as the same as the corresponding elements between two Bloch functions well inside the slab. The wave functions are determined by solving the eigenvalue problem represented by Eq. (18).

The Hamiltonian matrix elements were computed as functions of a two-dimensional wave vector (k_y,k_z) by choosing the same parameters as in the bulk calculation. The energy eigenvalues and the eigenstates were obtained by diagonalizing the Hamiltonian matrix, and the density of states as a function of energy is calculated using a statistical number of the eigenvalues. The density of states was normalized to give the proper number of orbitals per unit cell (which contains N silicon atoms for the unit cell in an N layer slab). Except for the intrinsic surface states, which lie in the band gap, the density of states calculated for a slab of a Si semiconductor (Fig. 4) is similar to the one obtained for the bulk silicon.

Since each primary unit cell of a bulk silicon crystal has two silicon atoms, one should include at least two layers of (100) plane in a superlayer in the application of the z-transform to a semi-infinite system. The $\mathbf{B}$ and $\mathbf{A}$ matrices, obtained by using the same solid state parameters as in the bulk and slab calculations, are all 8×8 matrices. The bulk and surface states of the semi-infinite semiconductor can both be obtained using the z-transform. A bulk state contains at least two propagating components and a surface state has only decaying wave functions.

In the experiments,[4] the electrode surfaces were occupied by hydrogen atoms to saturate the dangling bonds of surface silicon atoms, removing thereby the surface states resulted from the dangling bonds of the surface silicon atoms. According to previous calculations in the literature on a hydrogen-terminated Si (111) surface[32] all surface states were removed and the silicon–hydrogen interaction forms two bands deep inside the silicon bulk bands. Although the band structure of the hydrogen-terminated Si (100) slab is different, it seems reasonable to suppose that there will be no intrinsic surface states left for a perfect hydrogen-terminated Si (100) surface.

Downloaded 08 Mar 2006 to 131.215.225.174. Redistribution subject to AIP license or copyright, see http://jcp.aip.org/jcp/copyright.jsp

2. The electronic structure of the redox molecule

For the calculation of the rate constant of the electron transfer reaction at the silicon/viologen$^{2+/+}$ interfaces, N,N'-dimethyl-4,4$'$-bipyridylium^{2+} was chosen as the electron acceptor. Using the structural data of this cation in a crystal,[33] the most stable structure of the ion was obtained by the EHMACC (extended-Hückel molecular and crystal calculations program).[34] The two pyridyl planes formed thereby a 50^0 angle. However, since the calculation was performed without the consideration of the interactions between the acceptor and the solvent molecules, some differences may occur for the structure of this ion in solution. The LUMO of the ion, i.e., the acceptor state was obtained as a linear combination of the atomic orbitals,

$$\Phi=\sum_{i,j} C_{ij}\phi_{ij}, \tag{42}$$

where the sum is over the atoms i and the valence orbitals j of each atom with C_{ij}'s obtained from the extended-Hückel calculation.

3. Calculation of the electron transfer rate constant

To be consistent with the experiments where the only rate-limiting step is the electron transfer process the acceptors are considered homogeneously distributed in the solution. The orientations are taken as random, using 125 different orientations, each translated so as to have the closest pair of atoms, of the molecule and of the semiconductor surface, in van der Waals' contact, i.e., they have a separation distance equal to the sum of the atomic van der Waals' radii. The square of the electronic coupling is averaged over these orientations. In the calculations, the semiconductor is assumed to be uniform and is represented by the surface $x=0$, and the 125 orientations of the molecule are created by the rotations of the molecule in the three-dimensional space each with a set of randomly chosen Eulerian angles. The geometric center of the molecule with each selected orientation has 16 randomly chosen (y, z) coordinate relative to the closest Si surface atom. Because of the symmetry of the Si semiconductor surface, y and z vary between 0 and half a lattice constant. Under the assumption that the coupling decays exponentially with distance with a decay exponent β_s, the range of contributing distances is $1/\beta_s$, and we note that $\beta_s \approx 1$ Å^{-1}.[19] The averaged quantity of coupling matrix element, denoted by $\langle |V(\mathbf{k})|^2\rangle$ at the van der Waals' contact mentioned earlier was obtained by an extended-Hückel[34] calculation. For the hydrogen-terminated silicon surface, $\langle |V(\mathbf{k})|^2\rangle$ is calculated assuming a direct van der Waals' contact between the hydrogen atom on the Si surface and the closest atom of the redox species[35] for each given orientation. A certain number of states at each energy ϵ is randomly chosen to give the average of the square of the coupling, $\langle |\bar{V}(\epsilon)|^2\rangle$, which is then multiplied by the density of states to yield the total coupling at that energy.

Combining Eqs. (9), (13), and (16) an expression is obtained for the first-order electron transfer reaction rate constant,

TABLE I. Experimental and calculated $k_{et}^{\max}$.[a]

System	$k_{et}^{\max}$ (expt.)	$k_{et}^{\max}$ (*z-trans.*)	$k_{et}^{\max}$ (slab)
Si/viologen$^{2+/+}$	0.6[b]	1.3	1.6
InP/$Me_2Fc^{+/0}$	1–2[c]	0.084	0.086

[a]Units are 10^{-16} cm^4 s^{-1}, and the theoretical $k_{et}^{\max}$ includes only bulk states.
[b]From Ref. 4.
[c]From Ref. 1.

$$k_f=\frac{2\pi}{\hbar}\frac{1}{\sqrt{4\pi\lambda k_BT}}\frac{1}{\beta_s}\int_0^{\infty}\exp\left(-\frac{(\lambda+\Delta G^0-\epsilon)^2}{4\lambda k_BT}\right)\times\langle|\bar{V}(\epsilon)|^2\rangle f(\epsilon)\rho(\epsilon)d\epsilon, \tag{43}$$

where $\rho(\epsilon)$ and $\langle|\bar{V}(\epsilon)|^2\rangle$ are normalized to the unit cell. Because of the low occupancy of the semiconductor conduction band, and reflecting the Boltzmann factor the electron transfer can be regarded as occurring only near the edge of the conduction band, i.e., nearly at $\epsilon=0$. In Eq. (43) and hereinafter for convenience of discussion the energy ϵ of the electrons in the semiconductor will be referred to the conduction band edge at the semiconductor surface as zero.

For a semiconductor/electrolyte interface as in the electron transfer reaction studies in Refs. 1–6, the change of electrostatic potential across a semiconductor/liquid interface exists mainly within the semiconductor, because of the low concentration of the charge carriers in the semiconductor. In this case, the change of applied potential changes only the concentration of carriers at the interface and does not change the free energy ΔG^0 of the electron transfer reaction. As shown in the Appendix, the maximum second-order electron transfer rate constant can then be expressed as

$$k_{et}^{\max}=\frac{2\pi}{\hbar}\frac{1}{\sqrt{4\pi\lambda k_BT}}\frac{v}{\beta_s}\langle|\bar{V}|^2\rangle, \tag{44}$$

where $\langle|\bar{V}|^2\rangle$ is defined in the Appendix [cf. Eq. (A6)]. The maximum rate constant computed using the above equation is shown in Table I.

B. Indium phosphide/ferrocene interfaces

1. Band structure of indium phosphide

The bulk band structure of the InP semiconductor was calculated using the Hamiltonian and the interaction parameters given by Chadi *et al.*[24,36,37] The density of states computed for the bulk and a slab of the InP semiconductor are shown in Figs. 5 and 6, respectively. The electronic structure of Me_2Fc^+ was obtained from the extended-Hückel calculation[34] using the molecular structure given in Ref. 38. The electronic structure calculations were again performed for a slab and for a semi-infinite crystal model of the InP semiconductor with a (100) surface. The maximum second-order electron transfer rate constant (per unit area) was computed and the results are given in Table I.

Downloaded 08 Mar 2006 to 131.215.225.174. Redistribution subject to AIP license or copyright, see http://jcp.aip.org/jcp/copyright.jsp

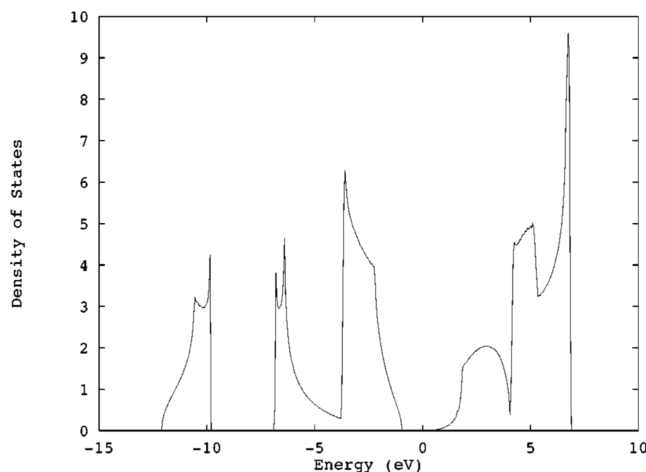

FIG. 5. Calculated density of states ρ for the bulk of InP semiconductor. The unit of the density of states is per unit cell (2 atoms) per eV. The Fermi level is located at 0 eV.

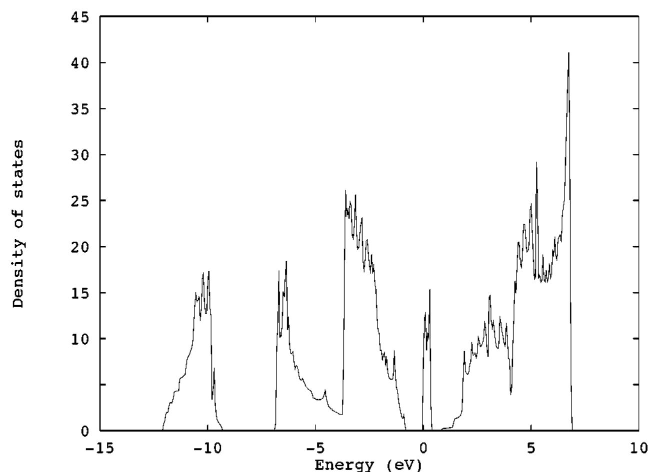

FIG. 6. Calculated density of states ρ for a slab of InP semiconductor. The unit of the density of states is per eV per unit cell. There are 20 atoms per unit cell, which has one atom on each face of the slab and so is 20 atoms thick. The Fermi level is located at 0 eV.

2. Contribution of surface states

Using considerations similar to those used in the treatment of bulk states we shall also assume that the electron transfer between a surface state and the bulk state is much faster than the electron transfer between the surface state and the molecular acceptor. In the preceding treatment we neglected the interactions which might lead to such a coupling, e.g., radiationless transitions. The resulting expression for the current density corresponding to the electron transfer from the surface states of the semiconductor to the acceptor is

$$J_f^{\mathrm{ss}}=e[A]\frac{2\pi}{\hbar}\frac{1}{\sqrt{4\pi\lambda k_BT}}\frac{1}{\beta_s}\times\int_\epsilon |V_{\mathrm{ss}}(\epsilon)|^2 e^{-[(\lambda+\Delta G)^2/4\lambda k_BT]}f(\epsilon)\rho_{\mathrm{ss}}(\epsilon)d\epsilon, \quad (45)$$

where ρ_{ss} is the density of surface states, and

$$\Delta G=\Delta G^0-\epsilon, \quad (46)$$

is the driving force for the electron transfer from a surface state with energy ϵ to the acceptor. If, for simplicity, it is further assumed that the surface states are distributed homogeneously in an energy range from $-\Delta E$ to 0, i.e., in an interval ΔE below the conduction band edge, then

$$\rho_{\mathrm{ss}}=\frac{N_{\mathrm{ss}}}{\Delta E}, \quad (47)$$

where N_{ss} is the total number of surface states.

The occupancy of these states obeys the Fermi–Dirac distribution,

$$f(\epsilon)=\frac{1}{1+e^{(\epsilon-\epsilon_f)/k_BT}}, \quad (48)$$

where ϵ_f is the Fermi level, and depends linearly on the applied potential E_{app},

$$\epsilon_f=eE_{\mathrm{app}}+\epsilon_f^0=eE_{\mathrm{app}}+V_{bi}^0+\epsilon_f^b. \quad (49)$$

Here, ϵ_f^0 is the value of ϵ_f when $E_{\mathrm{app}}=0$, V_{bi}^0 is the built-in voltage, the potential drop within the semiconductor, when $E_{\mathrm{app}}=0$, and ϵ_f^b is the energy difference between the Fermi level and the conduction band edge inside the semiconductor (Fig. 1). When any dependence of the coupling between the surface states and the acceptor state on the energy ϵ is neglected, an expression for the surface states contribution to the current density from the semiconductor to the acceptor state J_f^{ss} is

$$J_f^{\mathrm{ss}}=e[A]\frac{2\pi}{\hbar}\frac{1}{\sqrt{4\pi\lambda k_BT}}\frac{1}{\beta_s}\frac{N_{\mathrm{ss}}|V_{\mathrm{ss}}|^2}{\Delta E}\times\int_{-\Delta E}^0 e^{-[(\lambda+\Delta G)^2/4\lambda k_BT]}f(\epsilon)d\epsilon, \quad (50)$$

where ΔG is given by Eq. (46). Similarly, the current density due to the electron transfer from the donor to the surface states can be expressed as

$$J_b^{\mathrm{ss}}=-e[A^-]\frac{2\pi}{\hbar}\frac{1}{\sqrt{4\pi\lambda k_BT}}\frac{1}{\beta_s}\frac{N_{\mathrm{ss}}|V_{\mathrm{ss}}|^2}{\Delta E}\times\int_{-\Delta E}^0 e^{-[(\lambda-\Delta G)^2/4\lambda k_BT]}(1-f(\epsilon))d\epsilon. \quad (51)$$

The sum $J_f^{\mathrm{ss}}+J_b^{\mathrm{ss}}$ is next used to interpret the current-applied potential behavior obtained in the experiments. The $N_{\mathrm{ss}}|V_{\mathrm{ss}}|^2$ is treated as a single parameter which can be adjusted to fit the experimental data, in the absence of any other complicating factors.

3. Current vs applied potential behavior

As we have noted earlier, the total current can be written as the sum of two components,

$$J=J^{\mathrm{ss}}+J^{\mathrm{bk}}. \quad (52)$$

In the present treatment J^{ss} is computed using Eqs. (50) and (51) and J^{bk}, the current from the bulk states, is calculated using the tight-binding method.

Downloaded 08 Mar 2006 to 131.215.225.174. Redistribution subject to AIP license or copyright, see http://jcp.aip.org/jcp/copyright.jsp

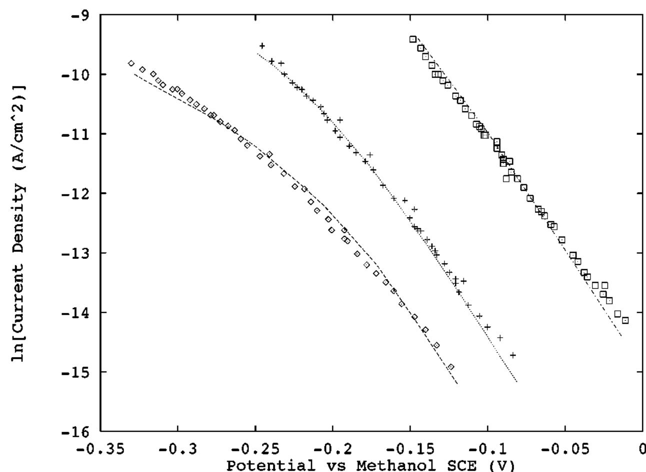

FIG. 7. Current-applied potential behavior at the $InP/Me_2Fe^{+/0}$ interfaces. The experimental data are taken from Ref. 1. From left to right, the concentrations of Me_2Fe^+ are 0.001 M, 0.01 M, 0.1 M, respectively. The concentration of Me_2Fe is 0.1 M. To fit the experimental data, $N_{ss}|V_{ss}|^2$ is taken as 1.25, 0.31, 0.44×10^{-8} eV^2, respectively.

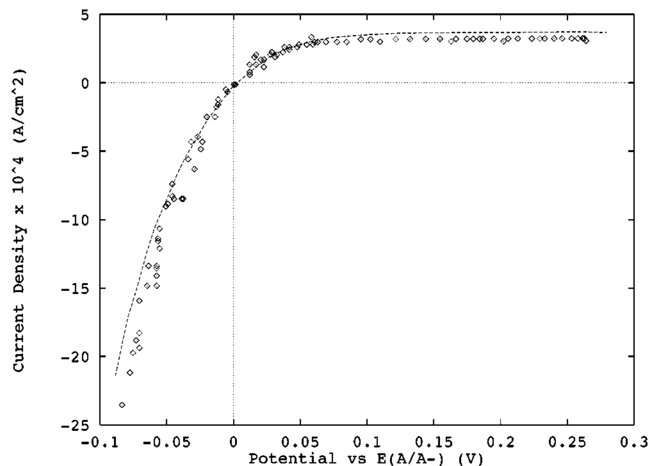

FIG. 8. Current-applied potential behavior at the $InP/PV^{2+/+}$ interfaces. The experimental data are taken from Ref. 1. $N_{ss}|V_{ss}|^2$ is taken as 3.2×10^{-8} eV^2.

When the current via the surface states dominates, namely, when the surface states are much more occupied than the conduction band or when the density of surface states is high, one has approximately for the forward and reverse current density,

$$J_f^{ss}+J_b^{ss}=0, \tag{53}$$

at equilibrium. In the case of the $InP/Me_2Fc^{+/0}$ interface, using Eqs. (48), (49), (50), (51), and (53) to fit the built-in voltage V_{bi}^0 of the semiconductor at zero applied potential, which leads to a equality between the integrals in Eqs. (50) and (51), a value for ΔE is obtained as 0.4 eV. This value of ΔE agrees with results from surface state studies of the (100) surface of lightly doped *n*-InP semiconductors in vacuum both experimentally[39] and theoretically,[40] where the surface states were shown to be located at (1/3) E_g below the conduction band minimum.[41] Here, E_g is the band gap of the semiconductor and is around 1.35 eV.

Similarly, the electrochemical studies at *p*-InP/electrolyte interfaces[42] also lead to surface states distributed mostly near the conduction band edge. Other parameters used in this calculation are as follows: the reorganization energy λ is 0.8 eV, as suggested in Ref. 1, ΔG^0 is 0.79 eV;[1] the parameter $N_{ss}|V_{ss}|^2$ is chosen as 10^{-8} $(eV)^2$ to fit the net current density obtained in the experiments[1] using Eqs. (50) and (51). The current density is then obtained as a function of the applied potential for different $[A]/[A^-]$ ratios and is compared with the experimental data. The curvature of the plot is determined by the relative position of the energy of the surface states and the Fermi level, and so depends on E_{app} and ΔG^0, as shown in Fig. 1. When the Fermi energy is much lower than the energies of the surface states, the occupancy of these states can be treated as obeying a Boltzmann distribution, and the $\ln[J]$ vs E_{app} curve is a straight line.[43] When the energy difference between the lowest surface states and the Fermi level is less than k_BT, the Fermi–Dirac distribution must be employed. The $\ln[J]$ vs E_{app} plot then deviates from a straight line, as shown in Fig. 7. In order to fit the experimental results different densities of states are used for different InP/liquid interfaces. This assumption is not necessarily correct, since the deviation of the horizontal distance between the neighboring curves in Fig. 7 from the value of 0.059 V may also result from experimental uncertainties.[44]

In order to fit the experimental current vs applied potential data obtained at the $InP/PV^{2+/+}$ interface by the diode equation,[1]

$$J=J_0(e^{-eE_{app}/Ak_BT}-1), \tag{54}$$

the A in Eq. (54) should be greater than 1.8, which indicates that the current vs applied potential behavior at this interface is far from ideal ($A=1$). A better fit is obtained by including surface states in the calculation, using the following parameters: $\Delta E=0.4$ eV, $\Delta G^0=-0.34$ eV,[1] $\lambda=0.5$ eV,[1] and $N_{ss}|V_{ss}|^2=2\times 10^{-8}$ $(eV)^2$. Here, ΔE is taken the same as in the $InP/Me_2Fc^{+/0}$ case and $N_{ss}|V_{ss}|^2$ is chosen to fit the measured net current density. The calculated result is shown in Fig. 8 together with the experimental results.

IV. DISCUSSION

The nonadiabatic description and the two-level approximation applied in our theoretical studies of electron transfer reactions at semiconductor/liquid interfaces provide a consistent value for the reaction rate constant when compared with the experimental results. Semiconductors differ from metals because of their band gap, which, as pointed out by Dogonadze,[11] makes the electron transfer reactions more likely to be nonadiabatic. This effect is associated with the low occupancy of the semiconductor conduction band, which allows the electron transfer to occur mainly nearly the edge of the conduction band. For a metal/liquid interface, the electron transfer reaction happens largely at the Fermi energy, and the coupling strength between the metal electrode and the molecular acceptor can be characterized by[15,22]

$$\Delta(\epsilon)=2\pi\sum_{\mathbf{k}} |V_{\mathbf{k}}|^2\delta(\epsilon_{\mathbf{k}}-\epsilon), \tag{55}$$

Downloaded 08 Mar 2006 to 131.215.225.174. Redistribution subject to AIP license or copyright, see http://jcp.aip.org/jcp/copyright.jsp

where $\Delta(\epsilon)$ is evaluated at the Fermi energy. $\Delta(\epsilon_f)/\hbar\omega_{\max}$ has been then taken[15,45] as the criterion for distinguishing nonadiabatic from adiabatic reactions for a metal/liquid interface,[15] where $\omega_{\max}$ is the ''fastest phonon mode'' contributing to the electron transfer reaction. For an $\omega_{\max}/2\pi$ of the order of $10^{13}\ \mathrm{s}^{-1}$ this $\hbar\omega_{\max}$ is about 0.03 eV. At a semiconductor/liquid interface, the electron transfer reaction occurs mainly near the edge of the conduction band. The interaction strength between the continuum states of a semiconductor and the acceptor state is better characterized by[20]

$$\Delta^I=\frac{1}{k_BT}\int_{\epsilon}\Delta(\epsilon)d\epsilon, \tag{56}$$

where the limit ''ϵ'' denotes a narrow interval of an amount k_BT at the semiconductor conduction band edge. Because of the low occupancy of the electronic states in the semiconductor conduction band, the electron transfer happens only at a small energy range near the conduction band edge, and then the important integration regime only covers a narrow interval of the order of k_BT. As pointed out by Harrison,[25] band energy is proportional to the square of $k-k_0$ near the conduction band edge, where k_0 is the value of k at the conduction band edge (conduction band minimum). The value of k_0 depends on the nature of the interaction of different bands. For InP k_0 is zero,[46] while for Si it is quite large.[46] For Si and InP, the density of states is very low near the conduction band edge,[25,46] the total coupling between these semiconductors and the molecular acceptor is typically weak. The Δ^I is the counterpart of the usual matrix element that appears in the two-state Landau-Zener formula. The present approximate calculations lead to a value of Δ^I of the order of 10^{-5} eV. In that case, with $\hbar\omega_{\max}\sim 0.03$ eV, the reactions can be regarded as nonadiabatic.

Since the double layer at the interface of semiconductor/liquid interfaces is neglected and the redox molecules are also allowed to penetrate to the electrode surface, the present calculations more likely represent an upper bound of the maximum rate constant. Although the approach in this study is intended to be a pragmatic one, the calculated result for the maximum rate constant at the Si/viologen$^{2+/+}$ interfaces is in a surprisingly reasonable agreement with the experimental data. The agreement for InP/$Me_2Fc^{+/0}$ is less satisfactory, the calculated value being approximately an order of magnitude smaller than the experimental one. Nevertheless, considering the approximation of using the extended-Hückel treatment to obtain the coupling, this extent of agreement is, in our opinion, encouraging.

The difference between the calculated results for Si/viologen$^{2+/+}$ and InP/$Me_2Fc^{+/0}$ systems[47] may be due to several effects. One factor is the difference in size of the acceptor state, since the LUMO of a viologen$^{2+/+}$ ion is calculated in the present work to be delocalized over the whole ring system, and the LUMO of a $Me_2Fc^{+/0}$ ion is localized mainly on the Fe^{3+} ion (here and in Ref. 48) and so distant from the periphery of the molecule. This effect would yield a larger electronic coupling between the semiconductor and the first redox species, other things being equal. However, there are factors which would make InP more effective than Si, e.g., a smaller effective electron mass,[25,46] and so tend to counter the above molecular effect. It would be useful therefore to study the two semiconductor systems with the same molecular species, if possible. In an effort to resolve this question using calculations we have compared the calculated maximum rate constant for the Si/viologen$^{2+/+}$ system, $1.6\times10^{-16}\ \mathrm{cm^4\,s^{-1}}$, as in Table I, with a maximum rate constant which we subsequently calculated for the Si/$Me_2Fc^{+/0}$ system, $0.17\times10^{-16}\ \mathrm{cm^4\,s^{-1}}$. Thus, it is seen that the viologen$^{2+/+}$ pair has a closer effective contact with the Si interface than does the $Me_2Fc^{+/0}$ pair. Accordingly, the experimental result in Table I, in contrast with the calculated results in that table, that the InP/$Me_2Fc^{+/0}$ has a higher rate than Si/viologen$^{2+/+}$, cannot be attributed to a more effective contact. For this reason we attribute the higher experimental rate for InP to the presence of surface states in the InP, as discussed earlier. We note also that the calculated (bulk state) result for InP/$Me_2Fc^{+/0}$ ($0.086\times10^{-16}\ \mathrm{cm^4\,s^{-1}}$) is comparable with the calculated (bulk state) result for Si/$Me_2Fc^{+/0}$ ($0.17\times10^{-16}\ \mathrm{cm^4\,s^{-1}}$).

Under some conditions, surface states may play a role in the electron transfer reactions at semiconductor/liquid interfaces, because of their localization at the electrode surfaces, as noted by previous authors.[9,16] Although the density of bulk states of the InP conduction band is large, of the order of $10^{17}\ \mathrm{cm}^{-3}$, the decay length of their coupling to the molecule of about 1 Å yields an effective surface density of states of the conduction band of the order of only $10^9\ \mathrm{cm}^{-2}$. We note further that in a free-electron model a surface state has a wave function which can be expressed as

$$\varphi\propto e^{-\beta_{ss}x}\cos(k_x x). \tag{57}$$

The $1/\beta_{ss}$ is about 8 Å for the InP semiconductor.[49] As a result, a large fraction of surface states can be effective in contributing to the electron tunneling event. In treating the electron transfer at InP/$Me_2Fc^{+/0}$ interfaces, the possibility of surface states was subsequently included in Sec. III B, as one interpretation of the nonideal current vs applied potential behavior in the experiments. A coupling strength between the surface states and the acceptor required to account for the discrepancy between the theoretical and experimental results was then estimated. We have not included any such contribution in Table I, the discrepancy in the rate constant of a factor of 10 between experimental and calculated results for the InP system in Table I could also have other sources.

While the inclusion of the surface states helps to explain the current vs applied potential behavior obtained in the experiments, the nonideal behavior being explained by the Fermi–Dirac occupancy of the surface states, the nonideal behavior can also result from many other mechanisms, such as the recombination of charge carriers in the solid bulk. The latter can produce a diode plot with a slope larger than unity.[50,51] We have noted earlier that the part of the present calculation which includes surface states is based on the assumption that the electron transfer between the bulk states and the surface states is much faster than the interfacial charge transfer, and is also based on a simplified model for the density of surface states. A deeper understanding of the mechanism would require the investigation of other pro-

Downloaded 08 Mar 2006 to 131.215.225.174. Redistribution subject to AIP license or copyright, see http://jcp.aip.org/jcp/copyright.jsp

cesses at the semiconductor/liquid interface and inside the semiconductor, as Anz and Lewis[50] have concluded from their recent simulation.

We turn next to a comparison of the electronic structure calculations of semiconductors with surfaces using the direct diagonalization vs using the z-transform. The direct diagonalization uses a slab of the crystal and mathematically is more straightforward, but because the computing time increases rapidly with the size of the slab, it is a less practical way to treat a very ''thick slab''. On the other hand, as noted in the literature,[52] usually a 20-layer slab is enough to produce a correct band structure for the crystal. The slab method is also a convenient method for obtaining the band structure and the density of states, and is practical for our purpose. With the z-transform method, a semi-infinite crystal is treated. Its mathematical formula is more complicated than that of the slab method, in that its solution requires the location of the roots of a high order and in many cases complex polynomial. Although it is time-consuming to obtain the whole band structure, in the application of the z-transform the energy is an input, the computing time can be considerably reduced if only states of some specific energies are required. The two methods provide similar results when they are applied to the calculations of the electron transfer reaction rate constants at semiconductor/liquid interfaces (Table I).

ACKNOWLEDGMENTS

It is a pleasure to acknowledge the support of the National Science Foundation and the Office of Naval Research. We thank Professor Nathan S. Lewis, Dr. Arnel M. Fajardo, and Samir J. Anz for valuable discussions, and Professors Mark Ratner and Harry Finklea for their especially helpful comments. We also thank Shachi S. Gosavi for discussions on the application of the z-transform method.

APPENDIX A: THE EXPRESSION FOR THE MAXIMUM ELECTRON TRANSFER RATE CONSTANT

As discussed in the text, in the integral in Eq. (43) $f(\epsilon)$ is the only term which depends on the applied potential E_{app},

$$f(\epsilon)=\exp\left(-\frac{\epsilon-\epsilon_f^0-eE_{\mathrm{app}}}{k_BT}\right), \tag{A1}$$

where the quantities in Eq. (A1) were defined earlier in the text [cf. Eq. (49)]. ϵ_f^0 is a constant for a semiconductor/liquid interface. Equation (43) can then be written as

$$k_f(E_{\mathrm{app}})=e^{eE_{\mathrm{app}}/k_BT}\frac{2\pi}{\hbar}\frac{1}{\sqrt{4\pi\lambda k_BT}}\frac{1}{\beta_s}\times\int_0^\infty \exp\left(-\frac{(\lambda+\Delta G^0-\epsilon)^2}{4\lambda k_BT}\right)\times\langle|\bar{V}(\epsilon)|^2\rangle f_0(\epsilon)\rho(\epsilon)d\epsilon, \tag{A2}$$

where $f_0(\epsilon)$ is the occupancy, $\exp[-(\epsilon-\epsilon_f^0)/k_BT]$, of the conduction band states at the semiconductor surface at zero applied potential. The number density of electrons n_s at the semiconductor surface is also a function of the applied potential,

$$n_s=n_0\exp\left(-\frac{eV_{\mathrm{bi}}^0-eE_{\mathrm{app}}}{k_BT}\right), \tag{A3}$$

where n_0 is the number density of conduction band electrons in the semiconductor bulk, and V_{bi}^0 is the potential drop within the semiconductor at zero applied potential, i.e., at $E_{\mathrm{app}}=0$.

Comparison of Eqs. (A2) and (A3) then illustrates that $k_f(E_{\mathrm{app}})$ is proportional to the density of surface electrons n_s. An expression of a second-order electron transfer rate constant that is independent of the applied potential, and thus of the density of surface electrons of the semiconductor, can be written as

$$k_{et}=\frac{2\pi}{n_0e^{-V_{bi}^0/k_BT}\hbar}\frac{1}{\sqrt{4\pi\lambda k_BT}}\frac{1}{\beta_s}\times\int_0^\infty \exp\left(-\frac{(\lambda+\Delta G^0-\epsilon)^2}{4\lambda k_BT}\right)\times\langle|\bar{V}(\epsilon)|^2\rangle f_0(\epsilon)\rho(\epsilon)d\epsilon. \tag{A4}$$

The $n_0e^{-V_{bi}^0/k_BT}$ in Eq. (A4) is readily evaluated, being equal to $\int\rho(\epsilon)f_0(\epsilon)d\epsilon/v$, with $\epsilon=0$ to $\epsilon=\infty$ as integration limits.[53] The v is the volume of the unit cell, and in the calculations using Eq. (A4) the wave functions are normalized to a unit cell.

Since we are interested in the maximum rate constant for the electron transfer, where $\lambda+\Delta G^0$ is nearly zero, in the exponent term of the free energy one can set $\epsilon=0$, since $\epsilon\ll\lambda$, and remove it from the integral, one then has

$$k_{et}=\frac{2\pi}{\hbar}\frac{1}{\sqrt{4\pi\lambda k_BT}}\frac{v}{\beta_s}\exp\left(-\frac{(\lambda+\Delta G^0)^2}{4\lambda k_BT}\right)\times\frac{\int_0^\infty\langle|\bar{V}(\epsilon)|^2\rangle f_0(\epsilon)\rho(\epsilon)d\epsilon}{\int_0^\infty f_0(\epsilon)\rho(\epsilon)d\epsilon}\cdot(\Delta G^0\simeq-\lambda). \tag{A5}$$

In the experiments,[4] the maximum rate constants were obtained by choosing a series of acceptors in the liquid with different reaction free energy but with similar reorganization energy around 0.7 eV.[4] Here, by setting $\Delta G^0+\lambda=0$, and by introducing an averaged coupling matrix element square,[53] $\langle|\bar{V}|^2\rangle$, where

$$\langle|\bar{V}|^2\rangle=\frac{\int_0^\infty\langle|\bar{V}(\epsilon)|^2\rangle f_0(\epsilon)\rho(\epsilon)d\epsilon}{\int_0^\infty f_0(\epsilon)\rho(\epsilon)d\epsilon}, \tag{A6}$$

an expression of the second-order electron transfer rate constant is then obtained as in Eq. (44).

[1] K. E. Pomykal and N. S. Lewis, J. Phys. Chem. B **101**, 2476 (1997).
[2] K. E. Pomykal, A. M. Fajardo, and N. S. Lewis, J. Phys. Chem. **100**, 3652 (1996).
[3] A. M. Fajardo and N. S. Lewis, Science **274**, 969 (1996).
[4] A. M. Fajardo and N. S. Lewis, J. Phys. Chem. B **101**, 11136 (1997).
[5] B. R. Horrocks, M. V. Mirkin, and A. J. Bard, J. Phys. Chem. **98**, 9106 (1994).

Downloaded 08 Mar 2006 to 131.215.225.174. Redistribution subject to AIP license or copyright, see http://jcp.aip.org/jcp/copyright.jsp

[6] I. Uhlendorf, R. Reineke-Kock, and R. Memming, J. Phys. Chem. **100**, 4390 (1996).
[7] R. A. Marcus, J. Phys. Chem. **95**, 1050 (1991).
[8] N. S. Lewis, Annu. Rev. Phys. Chem. **42**, 543 (1991).
[9] H. Gerischer, J. Phys. Chem. **95**, 1356 (1991).
[10] W. J. Royea, A. M. Fajardo, and N. S. Lewis, J. Phys. Chem. B **101**, 11152 (1997).
[11] R. R. Dogonadze and A. M. Kuznetsov, Prog. Surf. Sci. **6**, 42 (1975).
[12] R. A. Marcus, J. Phys. Chem. **94**, 1050 (1990).
[13] B. B. Smith and A. J. Nozik, Chem. Phys. **205**, 47 (1996).
[14] B. B. Smith, J. W. Halley, and A. J. Nozik, Chem. Phys. **205**, 245 (1996).
[15] W. Schmickler, J. Electroanal. Chem. **204**, 31 (1986).
[16] B. B. Smith and A. J. Nozik, J. Phys. Chem. B **101**, 2459 (1997).
[17] For examples, S. G. Davison and J. D. Levine, Solid State Phys. **25**, 1 (1970); D. J. Chadi and M. L. Cohen, Phys. Status Solidi B **68**, 405 (1975); Y. R. Yang and C. B. Duke, Phys. Rev. B **36**, 2763 (1987).
[18] R. A. Marcus, J. Chem. Phys. **98**, 5604 (1993).
[19] R. A. Marcus and N. Sutin, Biochim. Biophys. Acta **811**, 265 (1985).
[20] Y. D. Demkov and V. I. Osherov, Sov. Phys. JETP **26**, 916 (1968).
[21] H. Ou-Yang, B. Källebring, and R. A. Marcus, J. Chem. Phys. **98**, 7565 (1993).
[22] J. P. Muscat and D. M. Newns, Prog. Surf. Sci. **9**, 1 (1978).
[23] J. C. Slater and G. F. Koster, Phys. Rev. **94**, 1498 (1954).
[24] D. J. Chadi, Phys. Rev. B **16**, 790 (1977).
[25] W. A. Harrison, *Electronic Structure and the Properties of Solids* (Dover, New York, 1989).
[26] G. Allan, Surf. Sci. **299/300**, 319 (1994).
[27] D. H. Lee and D. Joannopoulos, Phys. Rev. B **23**, 4988 (1981).
[28] H. Ou-Yang, R. A. Marcus, and B. Källebring, J. Chem. Phys. **100**, 7814 (1994).
[29] D. A. Papaconstantopoulos, *Handbook of the Band Structure of Elemental Solids* (Plenum, New York, 1986).
[30] S. Gosavi and R. A. Marcus, J. Phys. Chem. B (to be published).
[31] S. T. Pantelides and J. Pollmann, J. Vac. Sci. Technol. **16**, 1349 (1979).
[32] F. Bechstedt and R. Enderlein, *Semiconductor Surfaces and Interfaces* (Akademie-Verlag, Berlin, 1988).
[33] J. H. Russell and S. C. Wallwork, Acta Crystallogr., Sect. B: Struct. Crystallogr. Cryst. Chem. **28**, 1527 (1971).
[34] M. H. Whangbo *et al.*, Extended Hückel Molecular, Crystal, and Properties Package, QCPE Program No. 571.
[35] The van der waals radii used in this study are taken from D. Freifelder, *Physical Chemistry for Students of Biology and Chemistry* (Science Books International, Boston, 1982), p. 60: H (1.2 Å), O (1.4 Å), and C (1.5 Å). The SiH (1.55 Å) and PO (1.84 Å) bond lengths are taken from D. F. Shriver, P. W. Atkins, and C. H. Langford, *Inorganic Chemistry* (Freeman and Company, New York, 1990), p. 68.
[36] D. J. Chadi, Phys. Rev. B **19**, 2074 (1979).
[37] D. J. Chadi and M. L. Cohen, Phys. Status Solidi B **68**, 405 (1975).
[38] J. D. Dunitz, L. E. Orgel, and A. Rich, Acta Crystallogr. **9**, 373 (1955).
[39] J. M. Moison, M. Van Rompay, and M. Bensoussan, Appl. Phys. Lett. **48**, 1362 (1986); J. M. Moison and M. Bensoussan, Surf. Sci. **168**, 68 (1986); S. S. Hullavarad, S. V. Bhoraskar, and D. N. Bose, J. Appl. Phys. **82**, 5597 (1997).
[40] B. C. Chan and C. K. Ong, J. Phys. Chem. Solids **52**, 699 (1991); W. G. Schmidt, Appl. Phys. A: Mater. Sci. Process. **65**, 581 (1997).
[41] Occupied surface states were also found at energy about 0.2 eV above the valence band maximum at 4×2 and 2×2 reconstructed *n*-InP (100) surfaces.[39,40] These surface states are energetically unfavorable in the electron transfer reactions considered in this study and are neglected in the calculations.
[42] H. J. Lewerenz, J. Electroanal. Chem. **356**, 121 (1993).
[43] When the Fermi energy is far below the energy of the surface states, the occupation of the surface states can be written as $f(\epsilon)=e^{-(\epsilon-\epsilon_f)/k_BT}$, where ϵ_f is given by Eq. (49). Since the $e^{-(\lambda+\Delta G)^2/4\lambda k_BT}$ term can be taken as a constant, Eq. (50) becomes $J_f^{ss}=e[A](2\pi/\hbar)(1/\sqrt{4\pi\lambda k_BT})(1/\beta_s)\quad(N_{ss}|V_{ss}|^2/\Delta E)\exp\{-[(\lambda+\Delta G_0+\Delta E)^2/4\lambda k_BT]\}\exp(-e(V_{bi}^0+\epsilon_f^b)/k_BT)\exp(-eE_{app}/k_BT)$. If J_f^{ss} is much lager than J_b^{ss}, $\ln J$ is linearly dependent on the applied potential E_{app} with a unit diode factor A, in Eq. (54).
[44] Lewis group (private communication),
[45] T. Iwasita, W. Schmickler, and J. W. Schultze, B. Bunsenges, Ber. Bunsenges. Phys. Chem. **89**, 138 (1985).
[46] Karl W. Böer, *Survey of Semiconductor Physics* (VNR, New York, 1990).
[47] The self-exchange electron transfer rate constant for the viologen system (S. Dai, thesis, University of Tennessee, 1990) is about one order higher than that of the Fc system [R. M. Neilson, G. E. MacManis, L. K. Safford, and M. J. Weaver, J. Chem. Phys. **93**, 2152(1989)]. Since no temperature-dependence measurement was done for the viologen system, the reorganization energy is unknown and thus no conclusion can be drawn by comparing the self-exchange reactions.
[48] G. L. Miessler and D. A. Tarr, *Inorganic Chemistry* (Prentice–Hall, New Jersey, 1999); A. Haaland, Acc. Chem. Res. **12**, 415 (1979); J. Giordan, J. H. Moore, and J. A. Tossel, *ibid.* **19**, 281 (1979); E. Rühl and A. P. Hitchcock, J. Am. Chem. Soc. **111**, 5069 (1989).
[49] W. Monch, *Semiconductor Surfaces and Interfaces* (Springer-Verlag, Berlin, 1993).
[50] S. J. Anz and N. S. Lewis, J. Phys. Chem. B **103**, 3908 (1999).
[51] S. J. Fonash, *Solar Cell Device Physics* (Academic, New York, 1981).
[52] I. Alstrup, Surf. Sci. **42**, 335 (1969).
[53] There is some arbitrariness of this definition of the surface density of electrons and the averaged coupling matrix element because the applied potential on different atom layers of the semiconductor are different. But because the coupling between the semiconductor atoms and the redox species decays fast with their distance (with a decay length in the order of 1 Å), and the applied potential varies slowly (with the band bending in the order of 100 nm), it is a good approximation to assume that the density of electrons is the same in the semiconductor surface region of present interest.

Downloaded 08 Mar 2006 to 131.215.225.174. Redistribution subject to AIP license or copyright, see http://jcp.aip.org/jcp/copyright.jsp